**GRAVITY FIELD OF THE ORIENTALE BASIN FROM THE GRAVITY RECOVERY AND INTERIOR LABORATORY (GRAIL) MISSION.** Maria T. Zuber[1], David E. Smith[1], Sander J. Goossens[2,] Jeffrey C. Andrews-Hanna[3], James W. Head[4], Walter S. Kiefer[5], Sami W. Asmar[6], Alexander S. Konopliv[6], Frank G. Lemoine[7], Isamu Matsuyama[8], Patrick J. McGovern[5], H. Jay Melosh[9], Gregory A. Neumann[7], Francis Nimmo[10], Roger J. Phillips[11], Sean C. Solomon[12, 13], G. Jeffrey Taylor[14], Michael M. Watkins[6], Mark A. Wieczorek[15], Brandon C. Johnson[1], James Keane[8], Katarina Miljković[1], Ryan S. Park[6], Jason M. Soderblom[1], David M. Blair[9], Erwan Mazarico[7], Dah-Ning Yuan[6]. [1]Department of Earth, Atmospheric and Planetary Sciences, Massachusetts Institute of Technology, Cambridge, MA 02129-4307, USA (zuber@mit.edu); [2]Center for Research and Exploration in Space Science and Technology, University of Maryland, Baltimore County, Baltimore, MD 21250, USA; [3]Deptarment of Geophysics, Colorado School of Mines, Golden, CO 80401, USA; [4]Department of Earth, Environmental and Planetary Sciences, Brown University, Providence, RI 02912, USA; [5]Lunar and Planetary Institute, Houston, TX 77058, USA; [6]Jet Propulsion Laboratory, California Institute of Technology, Pasadena, CA 91109-8099, USA; [7]NASA Goddard Space Flight Center, Greenbelt, MD 20771, USA; [8]Lunar and Planetary Laboratory, University of Arizona, Tucson, AZ 85721-0092, USA; [9]Department of Earth, Atmospheric, and Planetary Sciences, Purdue University, West Lafayette, IN 47907, USA; [10]Department of Earth and Planetary Sciences, University of California, Santa Cruz, CA 95064, USA; [11]Planetary Science Directorate, Southwest Research Institute, Boulder, CO 80302, USA; [12]Lamont-Doherty Earth Observatory, Columbia University, Palisades, NY 10964, USA; [13]Department of Terrestrial Magnetism, Carnegie Institution of Washington, Washington, DC 20015, USA; [14]Hawaii Institute of Geophysics and Planetology, University of Hawaii, Honolulu, HI 96822, USA; [15]Institut de Physique du Globe de Paris, Université Paris Diderot, 75205 Paris Cedex 13, France.

**Introduction:** During the final weeks (the "Endgame") of the Gravity Recovery and Interior Laboratory (GRAIL) mission [1], the orbital altitude of the dual spacecraft was lowered to an average of 11 km above the surface of the Moon. The Endgame mapping strategy [2] was designed to provide the highest-resolution coverage over the Orientale basin in order to yield a gravity map of a multi-ring impact basin at unprecedented resolution. (High-resolution data over other areas of the planet were acquired as well.) Here we present results of multiple global and local analyses to produce gravitational models with 3-5-km spatial resolution, appropriate for investigating the structure and evolution of Orientale and its surroundings. These independent solutions increase our confidence in interpreting features near the limits of resolution.

**Global Gravity Field Models with Focus on Orientale:** GRAIL [1], a twin spacecraft lunar gravity mission, was launched on September 10, 2012, and mapped the Moon at decreasing altitudes in sequential orbital phases, until its planned termination on December 17, 2012. Initial analysis of data acquired during the Primary Mission (PM) [3] at a mean orbital altitude of 55 km led to a global spherical harmonic model (GL0420A) of the gravitational field to degree and order 420 (spatial block size = 13 km) [4] that represented an improvement in spatial resolution by a factor of 3–4 and in quality by three to more than five orders of magnitude over previous models from all earlier missions. Subsequent PM spherical harmonic models reached degree and order 660 (spatial block size = 8.2 km) [5, 6]. During GRAIL's Extended Mission (XM), the mapping altitude was lowered by a factor of two to 23 km. The highest-resolution global gravity fields so far achieved from XM data at the NASA Goddard Space Flight Center and Jet Propulsion Laboratory, respectively, are to degree and order 1080 (spatial block size = 5 km) [7] and degree and order 1200 (spatial block size = 4.5 km) [8]. In practice these resolutions are achieved only at the lowest mapping altitudes. On December 6, 2012, the average altitude of the two GRAIL orbiters was lowered by another factor of two, to 11 km. This maneuver enabled a very-high-resolution mapping campaign over the Orientale basin (among other regions) during which time the twin spacecraft orbited to within 2 km of the surface of the basin's ring mountains.

**Local Solution for Orientale:** As an alternative approach to achieving very high resolution of Orientale, we derived a local model [9] based on a short-arc analysis [10] of GRAIL's Ka-band range-rate (KBRR) observations by adjusting *a priori* field GRGM900A while embedding neighbor smoothing [11, 12]. The local analysis removes high-frequency striping as well as extends the resolution of anomalies in Orientale and its environs to 3–5 km, suitable for detailed investigations of basin origin and evolution.

**Comparison with Previous Gravitational Field Models:** In previous analyses of the structure and compensation of Orientale [e.g., 13-16], the resolution of gravity was a limiting factor. In addition, it is now known that pre-GRAIL models under-sampled the Moon's gravitational power even at wavelengths that were then thought to be well resolved [cf. 4, 17].

**Crustal Structure:** Combination of GRAIL gravity with a 1/256° geodetically referenced topography [18] from the Lunar Orbiter Laser Altimeter (LOLA) [19] enables study of interior structure at the level of basin substructures. Subtracting the gravitational attraction of topography yields the Bouguer

gravity anomaly. Assuming for simplicity that the lunar crust and mantle are each of uniform density, Bouguer gravity can be downward continued to map the crust-mantle boundary to yield a map of crustal thickness. Although the assumption of uniform density is an approximation, its application to the regional crustal structure is supported by measurements of crustal density from GRAIL [20-22] as well as orbital remote sensing data. Although it has been suggested that the crust may be stratified into a mixed feldspathic layer overlying a layer of pure anorthosite [23], the density contrast between these rock types is small in comparison to the contrast across the crust-mantle interface.

Crustal thickness was determined using the approach of Wieczorek et al. [20], for a crustal density of 2550 kg $m^{-3}$ and a mantle density of 3220 kg $m^{-3}$, with a notable exception. Because the pre-existing crust was largely to entirely removed by the basin-forming impact [24], the crust at the basin center is likely dominated by the solidified impact melt sheet. There is a range of viewpoints regarding the extent and composition of the melt sheet related to the vertical extent of melting [25-28]. We assume a 10-km-thick melt sheet that spans Orientale's inner depression and adopt an average melt sheet bulk density of 2720 kg $m^{-3}$ based on the average bulk density measured for clast-poor lunar impact melt rocks [29]. The resulting structure, illustrated in Fig. 1, is characterized by a regional crustal thickness of 34 km and a crustal thickness beneath the basin depression of 12 km. The limiting case of no melt sheet would change the crustal thickness beneath the basin by less than 3 km.

The crustal thickness model shows a sharp transition between the basin excavation cavity and surrounding crust, with a 20–25° outward slope of the crust-mantle boundary surrounding the zone of mantle uplift. At smaller scale, azimuthal variations in crustal thickness correlate with Orientale's rings, and the rings are characterized by distinctive gravitational character that bear on structure and origin. These results are being used to constraint hydrocode models of Orientale and other basins [e.g., 30] and will inform the formation of basin-scale impacts and their role in the early evolution of lunar and other solid planetary crusts.

**References:** [1] Zuber M. T. et al. (2013) *Space Sci. Rev. 178,* 3-24, doi:10.1007/s11214-012-9952-7. [2] Sweetser T. H. et al. (2012) *AIAA Astrodyn. Specialist Conf.,* paper AIAA-2012-4429, Minneapolis, MN. [3] Roncoli R. B. and Fuji K.K. (2010) *AIAA Guidance, Navigation & Control Conf.,* paper *AIAA 2010-9393*, Toronto, Ontario, Canada. [4] Zuber M. T. et al. (2013) *Science 339,* 668-671, doi:10.1126/science.1231507. [5] Konopliv A. S. et al. (2013) *J. Geophys. Res. Planets 118,* 1415-1434, doi:10.1002/jgre.20097. [6] Lemoine F. G. et al. (2013) *J. Geophys. Res. Planets 118,* 1676-1698, doi:10.1002/jgre.20118. [7] Goossens S. J. et al. *AGU Fall Meeting,* abstract G22A-02. [8] Park R. S. et al. (2014) *AGU Fall Meeting,* abstract G22A-01. [9] Goossens S. et al. (2014) *Geophys. Res. Lett. 41,* 3367-3374, doi:10.1002/2014GL060178. [10] Rowlands D. D. et al. (2002) *J. Geod. 76,* 307-316. [11] Rowlands D. D. et al. (2010) *J. Geophys. Res. 115*, B01403, doi:10.1029/2009JB006546. [12] Sabaka T. J. et al. (2010) *J. Geophys. Res. 115,* B11403, doi:10.1029/2010JB007533. [13] Bratt S. R. et al. (1985) *J. Geophys. Res. 90,* 3049-3064, doi:10.1029/JB090iB04p03049. [14] Neumann G. A. et al. (1996) *J. Geophys. Res. 101*, 16,841-16,863. [15] von Frese R. B. et al. (1996) *J. Geophys. Res. 102,* 25,657-25,676. [16] Andrews-Hanna J. C. (2013) *Icarus 222,* 159-168, doi:10.1016/j.icarus.2012.10.031. [17] Namiki, N. et al. (2009) *Science 323,* 900-905, doi:10.1126/science.1168029. [18] Smith D. E. et al. (2010) *Geophys. Res. Lett. 37,* L18204, doi:10.1029/2010GL043751. [19] Smith D. E. et al. (2010) *Space Sci. Rev. 150,* 209-241, doi:10.1007/s11214-009-9512-y. [20] Wieczorek M. A. et al. (2013) *Science 339,* 671-675, doi:10.1126/science.1231530. [21] Han S.-C. et al. (2014) *Geophys. Res. Lett. 41,* 1882-1889, doi:10.1002/2014GL059378. [22] Besserer J. et al. (2014) *Geophys. Res. Lett. 41,* doi: 10.1002/2014GL060240. [23] Wieczorek M. A. et al. (2006) *Rev. Mineral. Geochem 60, 221-364,* doi:10.2138/rmg.2006.60.3. [24] Potter R. W. K. et al. (2013) *J. Geophys. Res. Planets 118,* 963-979, doi:10.1002/jgre.20080. [25] Vaughan W. M. et al., (2013) *Icrarus 223,* 749-765, doi: 10.1016/j.icarus.2013.01.017. [26] Spudis P. D. et al. (2014) *J. Geophys. Res. Planets 119,* 19-29, doi: 10.1002/2013JE004521. [27] Melosh H. J. et al. (2013) *Science 340,* 1552-1555, doi: 10.1126/science.1235768. [28] Freed A. M. et al. (2014) *J. Geophys. Res. Planets 119,* 2378-2397, doi: 10.1002/2014JE004657. [29] Kiefer W. S. et al. (2015) *Workshop on Early Solar System Bombardment,* Abstract #3004. [30] Johnson B. C. et al. (2015) *Lunar Planet Sci. 46,* this issue.

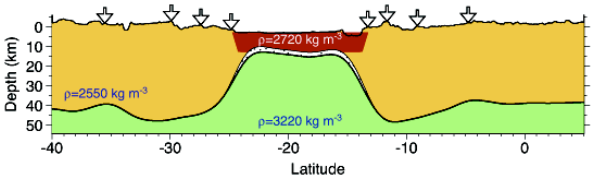


**Fig. 1.** Cross-section of Orientale's crustal structure from GRAIL and LOLA [18]. Brown corresponds to crust, green to mantle, and red to impact melt sheet. Arrows outward from center on each side correspond to locations of Inner Depression, Inner Rook Ring, Outer Rook Ring and Cordillera Ring.